



**HAL**  
open science

# Neural-Network-Based Fuzzy Observer with Data-Driven Uncertainty Identification for Vehicle Dynamics Estimation under Extreme Driving Conditions: Theory and Experimental Results

Cuong Nguyen, Anh-Tu Nguyen, Sebastien Delprat

► **To cite this version:**

Cuong Nguyen, Anh-Tu Nguyen, Sebastien Delprat. Neural-Network-Based Fuzzy Observer with Data-Driven Uncertainty Identification for Vehicle Dynamics Estimation under Extreme Driving Conditions: Theory and Experimental Results. IEEE Transactions on Vehicular Technology, In press, pp.1-11. 10.1109/TVT.2023.3249832 . hal-04017564

**HAL Id: hal-04017564**

**<https://uphf.hal.science/hal-04017564>**

Submitted on 7 Mar 2023

**HAL** is a multi-disciplinary open access archive for the deposit and dissemination of scientific research documents, whether they are published or not. The documents may come from teaching and research institutions in France or abroad, or from public or private research centers.

L'archive ouverte pluridisciplinaire **HAL**, est destinée au dépôt et à la diffusion de documents scientifiques de niveau recherche, publiés ou non, émanant des établissements d'enseignement et de recherche français ou étrangers, des laboratoires publics ou privés.

# Neural-Network-Based Fuzzy Observer with Data-Driven Uncertainty Identification for Vehicle Dynamics Estimation under Extreme Driving Conditions: Theory and Experimental Results

Cuong M. Nguyen, Anh-Tu Nguyen, *Senior Member, IEEE*, and Sébastien Delprat

**Abstract**—We present a neural network based Takagi-Sugeno (TS) fuzzy observer to estimate the lateral speed (or sideslip angle) of nonlinear vehicle dynamics subject to modeling uncertainties and unknown inputs. To this end, we first propose a TS fuzzy reduced-order observer design, which can be implemented with low computation effort, for nonlinear systems. The stability and robustness of the observer scheme against the modeling uncertainty is guaranteed by the  $\mathcal{H}_\infty$  filtering method. A data-driven approach is proposed to construct feedforward neural networks (NNs) for uncertainty approximation. This data-driven approach exploits a specific sliding mode observer (SMO) to identify the model uncertainty data from the collected training data. The NN-based uncertainty approximation is incorporated into the TS fuzzy observer structure to mitigate the effect of uncertainty and improve the estimation quality. Via Lyapunov's stability theory, design conditions of both the TS fuzzy reduced-order observer for dynamics estimation and the SMO for uncertainty identification are derived in terms of linear matrix inequalities. Experimental results obtained with the INSA autonomous vehicle on a real test track demonstrate the effectiveness of the proposed TS fuzzy observer under various driving scenarios. Performance comparisons are also performed to illustrate the interest of using NN-based uncertainty approximation for the new reduced-order observer scheme, especially under extreme driving conditions.

**Index Terms**—Vehicle dynamics, vehicle estimation, sideslip angle, nonlinear reduced-order observers, Takagi-Sugeno fuzzy systems, data-driven, neural networks.

## I. INTRODUCTION

Safety is one of the most important issues in vehicle engineering and research [1]. In many active safety applications deployed in vehicle systems, the lateral speed or sideslip angle plays a crucial role, *e.g.*, electronic stability control, vehicle lateral control, etc. [2]–[4]. However, commercial sensors used to measure the sideslip angle or lateral speed are too expensive to be equipped onboard in series-production vehicles [5]–[8]. This puzzle has captured the attention from the vehicle research community, which has culminated in a large number of publications on sideslip angle estimation [9]–[17]. Data

This work was supported in part by the French Ministry of Higher Education and Research, in part by the National Center for Scientific Research (CNRS); in part by the ANR HM-Science project (ANR-21-CE48-0021); in part by the Hauts-de-France Region under the project RITMEA 2021-2027.

C.M. Nguyen, A.-T. Nguyen and S. Delprat are with the laboratory LAMIH UMR CNRS 8201, Université Polytechnique Hauts-de-France, Valenciennes, France. A.-T. Nguyen and S. Delprat are also with the INSA Hauts-de-France, Valenciennes, France (e-mail: minhcuong86qn@gmail.com; tnguyen@uphf.fr; sebastien.delprat@uphf.fr).

fusion algorithms have been proposed to estimate the vehicle sideslip angle [18]–[21]. However, these methods lead to a high implementation complexity and cost issues. Hence, model-based methods have been widely developed for sideslip angle estimation [22]–[26].

Vehicle dynamics is nonlinear and complex by nature. It is difficult to identify a vehicle model, which is simple enough for control and observer designs while capturing well the vehicle dynamics under various operating conditions [2]. Accordingly, most model-based estimation methods only rely on some nominal vehicle models, *e.g.*, [12], [14], [22], [24]. A Takagi-Sugeno (TS) fuzzy unknown input observer is proposed in [22] to simultaneously estimate the lateral speed, the steering angle and the engine torque. A gradient descent based method is proposed in [12] to estimate the sideslip angle and the road friction. In [14], the sideslip angle is estimated by a kinematic based method. The steering angle and the sideslip angle are simultaneously estimated by a TS fuzzy observer in [24]. Since nominal vehicle models are only valid under simple driving scenarios, model-based methods can only perform well in limited situations. Hence, to improve the performance of these methods, it is crucial to improve the modeling quality.

Recent advances in machine learning methods have attracted particular interest from the control community. One of the most important tools in machine learning is artificial neural networks (NNs). Among different types of NNs, feedforward NNs are well-known for their universal capability of function approximation [27]. Many NN-based estimation methods have been reported in the literature where NNs are used to learn unknown dynamics [28]–[32]. A NN-based fault estimation method is developed in [29] for wind turbine systems. The authors in [30] propose a neuro-adaptive observer to estimate both vehicle states and tire forces. Multivariate deep recurrent NNs are used with long short-term memory units in [33] to estimate the brake pressure of electrified vehicles. An  $\mathcal{H}_\infty$  observer is developed in [34] to estimate the vehicle roll angle in presence of parameter uncertainties, where measurement of the pseudo-roll angle obtained by NNs.

Concerning the vehicle sideslip angle estimation, NN-based methods have been proposed where the vehicle models are not required [35]–[38]. For these model-free methods, different types of NNs are used to estimate the sideslip angle using onboard sensors as inputs and the sideslip angle as the output of developed NNs. In [39], the sideslip angle estimation is

performed using recurrent NNs together with a nonlinear Kalman filter. Recurrent NNs are combined with kinematic models to estimate the vehicle sideslip angle [40]. The main disadvantages of these NN-based estimation methods are concerned with the issues on stability, robustness to sensor noises, and the quantity as well as the quality of vehicle data used for NN training [9], [10]. Moreover, these methods may require a high computation effort [40]. Note that onboard computing units equipped in intelligent vehicles have to handle multiple tasks, *e.g.*, perception, planning and control, with limited capability. Hence, vehicle dynamics estimation should be carried out with low implementation and computation cost. Combining model-based and NN-based approaches, where NNs are exploited to approximate the vehicle uncertainties, can be promising to overcome these major drawbacks.

Motivated by the above analysis, this paper proposes a TS fuzzy reduced-order observer scheme to estimate the nonlinear vehicle dynamics subject to modeling uncertainties and unknown inputs. To this end, the vehicle nonlinear model is first represented by an equivalent TS fuzzy form. Then, an  $\mathcal{H}_\infty$  TS fuzzy reduced-order observer is designed for lateral speed estimation. The effect of uncertainty on the estimation error is alleviated by a NN-based uncertainty approximation, which is incorporated into the observer structure. A sliding mode observer (SMO) is utilized to identify the model uncertainty data from the training data. The model uncertainty data is used to train a feedforward neural network, whose inputs are the measured output and the control input of the vehicle, and the output is the approximated uncertainty. Backpropagation is used for the learning of the NN weights and biases with the training data collected in various driving situations. The main contributions of the paper are summarized as follows.

- We propose a new TS fuzzy observer design for a class of nonlinear uncertain systems subject to unknown inputs. The observer structure is of reduced order, which requires a low implementation cost in real-time.
- A data-driven approach is proposed to construct feedforward NNs for uncertainty approximation, where a specific sliding mode observer is used to identify model uncertainties from the training data. NN-based uncertainty approximation is incorporated into the observer structure to mitigate the uncertainty effect and improve the vehicle estimation quality under extreme driving conditions.
- The stability and robustness of the proposed NN-based observer scheme is guaranteed via Lyapunov stability theory. Design conditions of both TS fuzzy reduced-order observer for lateral speed estimation and SMO for NN-based uncertainty identification are obtained in terms of linear matrix inequalities (LMIs), which can be efficiently solved with numerical solvers.
- The practical performance of the proposed TS fuzzy reduced-order observer design is validated with an autonomous vehicle at our LAMIH-CNRS laboratory under various driving scenarios on a real test track. A comparative study is also performed to illustrate the superiority of the new result with respect to related works.

*Notation.* For a positive integer  $r$ , we denote  $\mathbb{I}_r =$

$\{1, 2, \dots, r\}$ . For a vector  $x$ ,  $x_i$  denotes its  $i$ th entry. For two vectors  $a, b \in \mathbb{R}^n$ :  $\text{co}(a, b) = \{\lambda a + (1 - \lambda)b : \lambda \in [0, 1]\}$  is the convex hull of  $a$  and  $b$ , and  $\text{col}\{a, b\} = [a^\top b^\top]^\top$ . For  $i \in \mathbb{I}_n$ :  $q_n(i) = [0, \dots, 0, 1_{i\text{th}}, 0, \dots, 0]^\top \in \mathbb{R}^n$  is a vector of the canonical basis of  $\mathbb{R}^n$ . For a matrix  $A$ ,  $A^\top$  denotes the transpose of  $A$ ,  $\text{He}(A) = A + A^\top$ . A positive definite matrix  $A$  is denoted by  $A \succ 0$ .  $\text{diag}(A_1, A_2)$  is the block-diagonal matrix composed of  $A_1, A_2$ . An identity matrix of dimension  $n$  is denoted by  $I_n$ , and a zero matrix of dimension  $m \times n$  is denoted by  $0_{m \times n}$ . The explicit dimensions of both identity and null matrices are omitted if straightforwardly deduced. Symbol  $\star$  represents the terms generated by symmetry in block matrices. Arguments are omitted when there is no confusion.

## II. VEHICLE MODELING AND PROBLEM FORMULATION

This section introduces the vehicle modeling and formulates the observer design problem for nonlinear uncertain systems subject to unknown inputs.

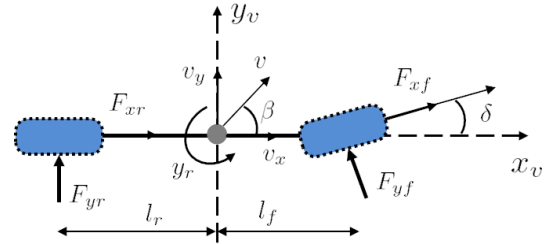


Fig. 1. Schematic of a two degrees-of-freedom vehicle model.

### A. Vehicle Nonlinear Model

We consider a two degrees-of-freedom vehicle model depicted in Fig. 1. Under regular driving conditions with small angles assumption and no longitudinal slip, the vehicle nonlinear dynamics can be described as [2], [22]

$$\begin{aligned} \dot{v}_y &= \frac{2(C_r l_r - C_f l_f) y_r - 2(C_f + C_r) v_y}{m_v v_x} - y_r v_x \\ &\quad + \frac{2C_f \delta}{m_v} - \frac{C_{dy} \rho_a A_{fy} v_y^2}{2m_v} \\ \dot{y}_r &= \frac{2(C_r l_r - C_f l_f) v_y - 2(C_f l_f^2 + C_r l_r^2) y_r}{I_z v_x} + \frac{2C_f l_f \delta}{I_z} \\ \dot{v}_x &= y_r v_y - \frac{C_{dx} \rho_a A_{fx} v_x^2}{2m_v} + \frac{T_w}{m_v R_t} \end{aligned} \quad (1)$$

where the vehicle parameters of the INSA autonomous vehicle at our LAMIH-CNRS laboratory are given in Table I.

The yaw rate  $y_r$  and the longitudinal speed  $v_x$  can be measured at low cost. However, the measurement of the lateral speed  $v_y$  is not online available due to expensive sensors. The steering angle  $\delta$  is the *known* control input  $u = \delta$ . Note that it is difficult to measure the wheel torque  $T_w$ , which is considered as an unknown input  $\omega = T_w$ . Then, the vehicle system (1) can be reformulated into the state-space form

$$\begin{aligned} \dot{x} &= A(z)x + f(x) + g(y, u) + W\omega \\ y &= Cx \end{aligned} \quad (2)$$

TABLE I  
VEHICLE PARAMETERS.

	Description	Value
$v_y$	Lateral speed	–
$v_x$	Longitudinal speed	–
$y_r$	Yaw rate	–
$\delta$	Front wheel steering angle	–
$T_w$	Longitudinal wheel torque force	–
$m_v$	Vehicle mass	1077 [kg]
$C_f$	Front cornering stiffness	47135 [N/rad]
$C_r$	Rear cornering stiffness	56636 [N/rad]
$l_f$	Distance between front axle and gravity center	1.08 [m]
$l_r$	Distance between rear axle and gravity center	1.24 [m]
$I_z$	Yaw moment of inertia	1442 [kgm <sup>2</sup> ]
$R_t$	Tire radius	0.26 [m]
$\rho_a$	Air density	1.23 [kg/m <sup>3</sup> ]
$C_{dy}$	Lateral drag coefficient	0.35 [–]
$C_{dx}$	Longitudinal drag coefficient	0.32 [–]
$A_{fy}$	Lateral frontal area	2.01 [m <sup>2</sup> ]
$A_{fx}$	Longitudinal frontal area	1.97 [m <sup>2</sup> ]

with  $x = [v_y \quad y_r \quad v_x]^\top$ ,  $z = [y_r \quad \frac{1}{v_x}]^\top$ , and

$$A(z) = \begin{bmatrix} -\frac{2(C_f+C_r)}{m_v v_x} & \frac{2(C_r l_r - C_f l_f)}{m_v v_x} & -y_r \\ \frac{2(C_r l_r - C_f l_f)}{I_z v_x} & -\frac{2(C_f l_f^2 + C_r l_r^2)}{I_z v_x} & 0 \\ y_r & 0 & 0 \end{bmatrix}$$

$$f(x) = \begin{bmatrix} -\frac{C_{dy} \rho_a A_{fy} v_y^2}{2m_v} \\ 0 \\ 0 \end{bmatrix}, \quad g(y, u) = \begin{bmatrix} \frac{2C_f \delta}{I_z} \\ \frac{m_v y_r \delta}{I_z} \\ -\frac{C_{dx} \rho_a A_{fx} v_x^2}{2m_v} \end{bmatrix}$$

$$W = \begin{bmatrix} 0 \\ 0 \\ \frac{1}{m_v R_t} \end{bmatrix}, \quad C = \begin{bmatrix} 0 & 1 & 0 \\ 0 & 0 & 1 \end{bmatrix}.$$

Since  $y_r$  and  $v_x$  can be measured at low cost, they are available as output measurements  $y = Cx$  in system (2). Due to the nonlinear nature of the vehicle model (1), the state-space matrix  $A(z)$  in (2) is time-varying rather than constant. The choice of  $z = [y_r \quad \frac{1}{v_x}]^\top$  is due to the fact that  $y_r$  and  $v_x$  are measurable, which later allows to equivalently represent system (3) by the TS fuzzy model (8) for observer design.

System (2) represents the nominal vehicle dynamics, whose front and rear tire forces are respectively modeled using the following linear model:

$$F_f = 2C_f \alpha_f, \quad F_r = 2C_r \alpha_r$$

where  $\alpha_f$  and  $\alpha_r$  are front and rear wheels slip angles. Note that the cornering stiffness coefficients  $C_f$  and  $C_r$  as well as the yaw moment of inertia  $I_z$  cannot be accurately identified in practice [24]. Only nominal values of  $C_f$ ,  $C_r$  and  $I_z$  can be provided as in Table I. Hence, modeling errors and uncertainties should be taken into account in the observer design for an effective vehicle dynamics estimation.

### B. Problem Formulation

A generic formulation of the nonlinear dynamics (2) with unknown input and uncertainty is considered as follows:

$$\begin{aligned} \dot{x} &= A(z)x + f(x) + g(y, u) + W\omega + d \\ y &= Cx, \quad x \in \mathcal{D} \end{aligned} \quad (3)$$

where  $\mathcal{D}$  is a state-space compact set,  $x \in \mathbb{R}^n$  is the state vector,  $u \in \mathbb{R}^{n_u}$  is the known input,  $y \in \mathbb{R}^p$  is the output vector,  $z \in \mathbb{R}^{n_z}$  is the vector of measurable premise variables,  $f(x)$  and  $g(y, u) \in \mathbb{R}^n$  are nonlinearities,  $\omega \in \mathbb{R}^{n_\omega}$  is the unknown input, and  $d \in \mathbb{R}^n$  represents the *lumped modeling uncertainties*. The known constant matrices  $W \in \mathbb{R}^{n \times n_\omega}$  and  $C \in \mathbb{R}^{p \times n}$  are full column rank and full row rank, respectively, which satisfy

$$\text{rank}(CW) = \text{rank}(W). \quad (4)$$

**Remark 1.** Under condition (4), a coordinate transformation  $\mathcal{T}$  can be constructed for system (3) such that  $C$  and  $W$  are in the following form [41]:

$$C = [0_{p \times (n-p)} \quad I_p], \quad W = \begin{bmatrix} 0_{(n-p) \times n_\omega} \\ W_p \end{bmatrix} \begin{matrix} \updownarrow n-p \\ \updownarrow p \end{matrix}. \quad (5)$$

Hence, without loss of generality, we consider in the sequel system (3) where  $C$  and  $W$  are in the form (5).

The nonlinearity  $f(x)$  satisfies the following assumption.

**Assumption 1.** The nonlinear function  $f(x)$  is differentiable with respect to  $x$  and satisfies

$$\underline{f}_{ij} \leq \frac{\partial f_i}{\partial x_j}(x) \leq \bar{f}_{ij}, \quad i, j \in \mathbb{I}_n \quad (6)$$

with  $\underline{f}_{ij} = \min_{\check{x} \in \mathcal{D}} \left( \frac{\partial f_i}{\partial x_j}(\check{x}) \right)$ , and  $\bar{f}_{ij} = \max_{\check{x} \in \mathcal{D}} \left( \frac{\partial f_i}{\partial x_j}(\check{x}) \right)$ .

**Remark 2.** Assumption 1 is necessary for the implementation of the differential mean value theorem stated in Lemma 1 in Section III. This instrumental allows to reformulate the mismatching nonlinear term involved the estimation error dynamics (26). Accordingly, robust stability analysis of the estimation error system (12)–(28) can be investigated, and LMI conditions can be derived for observer design.

Neural networks are well-known for the universal approximation capability. Hence, we assume that the uncertainty  $d$  can be approximated by a feedforward neural network  $\eta(y, u)$  as

$$d = \eta(y, u) + e_\eta \quad (7)$$

where  $e_\eta$  is the NN approximation error. The neural network  $\eta(y, u)$  is used to alleviate the effect of the uncertainty  $d$  on the estimation error. A data-driven approach to learn  $\eta(y, u)$  is presented in Section IV.

**Remark 3.** The neural network  $\eta(y, u)$  in (7) only depends on the measured signals as inputs, *i.e.*,  $y$  and  $u$ , which simplifies the observer design for the nonlinear uncertain system (3).

Applying the sector nonlinearity approach [42, Chapter 2] with premise variables vector  $z$  and  $x \in \mathcal{D}$ , system (3) can be *equivalently* represented by the following TS fuzzy model:

$$\begin{aligned} \dot{x} &= \sum_{i=1}^m \rho_i(z) A_i x + f(x) + \eta_g(y, u) + W\omega + e_\eta \\ y &= Cx, \quad m = 2^{n_z} \end{aligned} \quad (8)$$

where  $A_i$  are local constant matrices, and

$$\eta_g(y, u) = \eta(y, u) + g(y, u).$$

The membership functions  $\rho_i(z)$ ,  $i \in \mathbb{I}_m$ , satisfy the convex sum property, *i.e.*,  $\rho_i(z) \geq 0$ , and  $\sum_{i=1}^m \rho_i(z) = 1$ .

The structure of the proposed NN-based TS fuzzy reduced-order observer is depicted in Fig. 2. This paper addresses the following NN-based fuzzy observer design problem.

**Problem 1.** Determine a TS fuzzy reduced-order observer, where the effect of the uncertainty  $d$  on the estimation error is mitigated by a feedforward neural network (7), to estimate the state vector  $x$  of system (3).

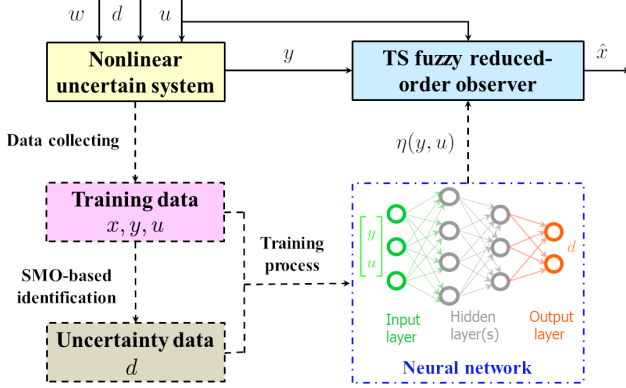


Fig. 2. Takagi-Sugeno fuzzy reduced-order observer structure with NN-based uncertainty identification (solid line: online computation, dashed line: offline computation).

### III. REDUCED-ORDER OBSERVER DESIGN

This section presents a reduced-order observer design with guaranteed  $\mathcal{H}_\infty$  robustness against uncertainty. Let us consider the following reduced-order observer for system (8):

$$\begin{aligned} \dot{\xi} &= \sum_{i=1}^m \rho_i(z)(E_i \xi + F_i y) + Gf(\hat{x}) + G\eta_g(y, u) \\ \hat{x} &= M\xi + Ny \end{aligned} \quad (9)$$

where  $\hat{x} \in \mathbb{R}^n$  is the estimate of  $x$ ,  $\xi \in \mathbb{R}^{n-p}$  is the state vector of the reduced-order observer, the observer matrices  $E_i$ ,  $F_i$  ( $i \in \mathbb{I}_m$ ),  $G$ ,  $M$  and  $N$  are to be designed such that

$$MG + NC = I \quad (10)$$

$$E_i G + F_i C = GA_i, \quad i \in \mathbb{I}_m. \quad (11)$$

Define  $e = x - \hat{x}$ , and  $\varepsilon = Gx - \xi$ . It follows from (8), (9), (10) and (11) that

$$e = (MG + NC)x - (M\xi + NCx) = M\varepsilon \quad (12)$$

$$\begin{aligned} \dot{e} &= \sum_{i=1}^m \rho_i(z)(E_i G + F_i C)x + Gf(x) + G\eta_g(y, u) + GW\omega \\ &\quad + Ge_\eta - \sum_{i=1}^m \rho_i(z)((E_i \xi + F_i y) + Gf(\hat{x}) + G\eta_g(y, u)) \\ &= \sum_{i=1}^m \rho_i(z)E_i \varepsilon + G\Delta f + GW\omega + Ge_\eta \end{aligned} \quad (13)$$

with  $\Delta f = f(x) - f(\hat{x})$ .

To design  $G$ ,  $M$ ,  $N$ ,  $E_i$  and  $F_i$ ,  $i \in \mathbb{I}_m$ , such that equations (10) and (11) hold, we choose a matrix  $H \in \mathbb{R}^{(n-p) \times n}$  such that  $[H^\top \quad C^\top]^\top$  is nonsingular and define

$$G = H - LC \quad (14)$$

where  $L$  is a gain matrix to be determined. Then, it follows from (14) that

$$\begin{bmatrix} G \\ C \end{bmatrix} = \begin{bmatrix} I & -L \\ 0 & I \end{bmatrix} \begin{bmatrix} H \\ C \end{bmatrix} \quad (15)$$

which means that  $[G^\top \quad C^\top]^\top$  is also nonsingular. Accordingly, equation (10) can be rewritten as

$$[M \quad N] = \begin{bmatrix} G \\ C \end{bmatrix}^{-1}. \quad (16)$$

From (15) and (16), the matrix  $M$  can be computed as

$$\begin{aligned} M &= \begin{bmatrix} G \\ C \end{bmatrix}^{-1} \begin{bmatrix} I_{n-p} \\ 0 \end{bmatrix} = \begin{bmatrix} H \\ C \end{bmatrix}^{-1} \begin{bmatrix} I & L \\ 0 & I \end{bmatrix} \begin{bmatrix} I_{n-p} \\ 0 \end{bmatrix} \\ &= \begin{bmatrix} H \\ C \end{bmatrix}^{-1} \begin{bmatrix} I_{n-p} \\ 0 \end{bmatrix} \end{aligned} \quad (17)$$

which means that  $M$  can be determined after choosing  $H$ . Meanwhile,  $N$  is computed from (16) as

$$N = \begin{bmatrix} G \\ C \end{bmatrix}^{-1} \begin{bmatrix} 0 \\ I_p \end{bmatrix}. \quad (18)$$

Furthermore, equation (11) can be rewritten as

$$[E_i \quad F_i] \begin{bmatrix} G \\ C \end{bmatrix} = GA_i, \quad \forall i \in \mathbb{I}_m. \quad (19)$$

From (16) and (19), we can obtain

$$E_i = GA_i M, \quad F_i = GA_i N, \quad \forall i \in \mathbb{I}_m. \quad (20)$$

Note that the algebraic equations (10) and (11) hold if  $M$ ,  $N$ ,  $E_i$  and  $F_i$ , for  $i \in \mathbb{I}_m$ , are designed by (17), (18), and (20). To determine  $G$  from (14), since the matching condition (4) holds, it follows that

$$\text{rank}(CW) = \text{rank} \begin{bmatrix} HW \\ CW \end{bmatrix}.$$

Let us select

$$L = HW(CW)^+ + Z(I_p - (CW)(CW)^+) \quad (21)$$

where  $(CW)^+$  is the pseudo-inverse of  $CW$  and  $Z$  is the observer gain matrix to be designed, and denote

$$R = H - HW(CW)^+ C, \quad (22)$$

$$S = [I_p - (CW)(CW)^+] C. \quad (23)$$

Then, from (14) and (21), we have

$$G = R - ZS \quad (24)$$

and

$$LCW = HW \Leftrightarrow GW = 0. \quad (25)$$

From (13), (20), (24) and (25), system (13) is rewritten as

$$\dot{e} = \sum_{i=1}^m \rho_i(z)(R - ZS)A_i M \varepsilon + (R - ZS)\Delta f + (R - ZS)e_\eta \quad (26)$$

where  $Z$  is designed to stabilize the system formed by (12) and (26). Accordingly,  $G$  can be determined from (24).

The following differential mean value theorem is useful to reformulate the nonlinear term  $\Delta f$  in (26) as a function of the estimation error  $\varepsilon$ .

**Lemma 1** ([43]). Let  $f(x) : \mathbb{R}^n \rightarrow \mathbb{R}^n$  and  $a, b \in \mathbb{R}^n$ . If  $f(x)$  is differentiable with respect to  $x$  on  $\text{co}(a, b)$ , there exist vectors  $c_i \in \text{co}(a, b)$ ,  $c_i \neq a$ ,  $c_i \neq b$ , for  $i \in \mathbb{I}_n$ , such that

$$f(a) - f(b) = \left( \sum_{i=1}^n \sum_{j=1}^n \varrho_n(i) \varrho_n^\top(j) \frac{\partial f_i}{\partial x_j}(c_i) \right) (a - b).$$

Applying Lemma 1 under Assumption 1, we rewrite  $\Delta f$  as

$$\Delta f = \mathcal{A}_f(x - \hat{x}) = \mathcal{A}_f M \varepsilon \quad (27)$$

where  $\mathcal{A}_f = \sum_{i=1}^n \sum_{j=1}^n \varrho_n(i) \rho_n^\top(j) \frac{\partial f_i}{\partial x_j}(\check{x}_i)$ ,  $\check{x}_i \in \text{co}(x, \hat{x})$ , is a matrix with parameters varying in a bounded convex set  $\mathcal{H}_f$ . Under Assumption 1, the vertices set of  $\mathcal{H}_f$  is given by

$$\mathcal{V}_{\mathcal{H}_f} = \left\{ \theta = (\theta_{ij}) \in \mathbb{R}^{n \times n} : \theta_{ij} \in \left\{ \underline{f}_{ij}, \bar{f}_{ij} \right\} \right\}$$

where  $\underline{f}_{ij}$  and  $\bar{f}_{ij}$  are as in (6). Then, it follows from (26) and (27) that

$$\dot{\varepsilon} = \sum_{i=1}^m \rho_i(z) (R - ZS)(A_i + \mathcal{A}_f) M \varepsilon + (R - ZS) e_\eta. \quad (28)$$

To stabilize the estimation error system (12)-(28),  $\mathcal{H}_\infty$  filtering approach is used to design  $Z$  such that

$$\Omega = \dot{V}(\varepsilon) + e^\top e - \gamma^2 e_\eta^\top e_\eta < 0 \quad (29)$$

where  $V(\varepsilon) = \varepsilon^\top P \varepsilon$ , with  $P \succ 0$ , is a Lyapunov function candidate, and  $\gamma > 0$  is the disturbance attenuation level. The following theorem provides LMI-based conditions to guarantee condition (29) with a minimal value of  $\gamma$ .

**Theorem 1.** Condition (29) for the estimation error dynamics (12)-(28) is guaranteed while minimizing  $\gamma$  if there exist matrices  $P \succ 0$ ,  $X$  of appropriate dimensions, and a scalar  $\bar{\gamma} > 0$  that solve the convex optimization problem:

$$\begin{aligned} \min(\bar{\gamma}) \quad & \text{subject to} \\ \Pi_i = & \begin{bmatrix} \text{He}(\Lambda_i) + M^\top M & PR - XS \\ * & -\bar{\gamma}I \end{bmatrix} < 0 \end{aligned} \quad (30)$$

with  $\Lambda_i = (PR - XS)(A_i + \mathcal{A}_f)M$ , for  $i \in \mathbb{I}_m$ , and  $\forall \mathcal{A}_f \in \mathcal{V}_{\mathcal{H}_f}$ . Moreover, the gain matrix  $Z$  is obtained as  $Z = P^{-1}X$ , and the minimal  $\gamma$  is computed as  $\gamma = \sqrt{\bar{\gamma}}$ .

*Proof.* Computing the time-derivative of  $V(\varepsilon)$  along the solution of system (28) and using expression (12), then the expression of  $\Omega$  in (29) can be rewritten as

$$\begin{aligned} \Omega = & \dot{V}(\varepsilon) + e^\top e - \gamma^2 e_\eta^\top e_\eta \\ = & 2\varepsilon^\top \left\{ \sum_{i=1}^m \rho_i(z) (PR - PZS)(A_i + \mathcal{A}_f) M \varepsilon \right. \\ & \left. + (PR - PZS) e_\eta \right\} + \varepsilon^\top M^\top M \varepsilon - \gamma^2 e_\eta^\top e_\eta. \end{aligned} \quad (31)$$

Denote  $X = PZ$ ,  $\bar{\gamma} = \gamma^2$ , and  $\zeta = \text{col}\{\varepsilon, e_\eta\}$ , it follows from (31) that  $\Omega = \sum_{i=1}^m \rho_i(z) \zeta^\top \Pi_i \zeta$ . Thus, condition (29) holds if (30) holds. Furthermore,  $\gamma$  is minimized by minimizing  $\bar{\gamma}$ .  $\square$

The procedure to design the matrices  $E_i, F_i, G, M, N$  for the reduced-order observer (9) is summarized in Algorithm 1.

---

**Algorithm 1:** Reduced-order observer design

---

- 1 Choose a matrix  $H$  such that  $[H^\top \ C^\top]^\top$  is nonsingular.
  - 2 Compute  $M$  by (17),  $R$  by (22) and  $S$  by (23).
  - 3 Determine the observer gain  $Z$  with Theorem 1.
  - 4 Compute  $G$  by (24).
  - 5 Compute  $N$  by (18).
  - 6 Compute  $E_i$  and  $F_i$  by (20).
- 

**Remark 4.** Note that there always exists a matrix  $H$  such that  $[H^\top \ C^\top]^\top$  is nonsingular [44]. For example, since  $C = [0 \ I_p]$ , we can choose  $H = [I_{n-p} \ 0]$ . Thus, the existence of the reduced-order observer (9) is guaranteed by condition (4) and the solvability of (30).

#### IV. DATA-DRIVEN APPROACH FOR NN-BASED UNCERTAINTY APPROXIMATION

This section presents a data-driven approach for neural-network-based uncertainty approximation, where  $\eta(y, u)$  in (7) is trained to alleviate the effect of  $d$  on the estimation error  $e$ .

##### A. System Partition

Since  $C$  and  $W$  are in the form (5), by reordering the last  $p$  components of the state vector  $x$ , without loss of generality,  $W_p$  can be further written in the form

$$W_p = \begin{bmatrix} 0 \\ W_q \end{bmatrix} \begin{array}{l} \uparrow p-q \\ \downarrow q \end{array} \quad (32)$$

where all the rows of  $W_q$  are non-zeros. We assume that  $W_q$  is full row rank, *i.e.*,  $\text{rank}(W_q) = q$ . By choosing  $H = [I_{n-p} \ 0_{(n-p) \times p}]$ , since  $C$  and  $W$  respectively are in the form (5) and (32), it follows that  $HW(CW)^+C = 0$ , or

$$R = H - HW(CW)^+C = [I_{n-p} \ 0_{(n-p) \times p}]. \quad (33)$$

Moreover, since  $W_q$  is assumed to be full row rank, it follows that  $(CW)(CW)^+ = \text{diag}\{0_{(p-q) \times (p-q)}, I_q\}$ , or

$$\begin{aligned} S = & [I_p - (CW)(CW)^+]C \\ = & \begin{bmatrix} 0_{p \times (n-p)} & \text{diag}\{I_{p-q}, 0_{q \times q}\} \end{bmatrix}. \end{aligned} \quad (34)$$

Then, it follows from (33) and (34) that the last  $q$  columns of  $G = R - ZS$  are zeros. Accordingly, the last  $q$  rows of  $e_\eta$  are canceled in  $(R - ZS)e_\eta$  and do not affect the estimation error dynamics (12)–(28). In other words, it is not necessary to find a neural network approximation for the last  $q$  components of

the uncertainty vector  $d$ . Let us partition  $d$ ,  $x$ ,  $f(x)$ ,  $g(y, u)$ ,  $A_i$  as follows:

$$\begin{aligned} d &= \begin{bmatrix} d_d \\ d_q \end{bmatrix}, \quad x = \begin{bmatrix} x_d \\ x_q \end{bmatrix}, \quad f(x) = \begin{bmatrix} f_d(x) \\ f_q(x) \end{bmatrix} && \begin{matrix} \updownarrow n-q \\ \updownarrow q \end{matrix} \\ g(y, u) &= \begin{bmatrix} g_d(y, u) \\ g_q(y, u) \end{bmatrix}, \quad A_i = \begin{bmatrix} A_{idd} & A_{idq} \\ A_{iqd} & A_{iqq} \end{bmatrix} && \begin{matrix} \updownarrow n-q \\ \updownarrow q \end{matrix} \end{aligned}$$

with  $d_q, x_q, f_q(x), g_q(y, u) \in \mathbb{R}^q$  and  $A_{iqq} \in \mathbb{R}^{q \times q}$ . Note that

$$W = \begin{bmatrix} 0 \\ W_q \end{bmatrix} \begin{matrix} \updownarrow n-q \\ \updownarrow q \end{matrix}.$$

Then, it follows from (3) and (5) that

$$\dot{\hat{x}}_d = \sum_{i=1}^m \rho_i(z) (A_{idd} \hat{x}_d + A_{idq} x_q) + f_d(x) + g_d(y, u) + d_d \quad (35)$$

where  $d_d$  is to be approximated by a neural network.

**Remark 5.** To alleviate the effect of the uncertainty  $d$  on the estimation error  $e$ , instead of approximating  $d$ , it is only required to approximate  $d_d$ . Note that since  $\omega$  is not involved in the dynamics (35), the SMO (36) can be designed for (35) for the identification of  $d_d$  in the training data.

### B. SMO-Based Uncertainty Identification for Training Data

To train a neural network for uncertainty approximation, the data of the state vector, control input, and measured output of system (3) are collected in various operating conditions. The following assumption is considered for collected vehicle data.

**Assumption 2.** In the collected data used to train the neural network for uncertainty approximation, the *offline* full-state information of the vehicle is available.

This assumption is reasonable in practice since despite the unavailability of onboard information of  $v_y$  due to sensors cost reasons (therefore, the vehicle state estimation is required for practical uses), such vehicle sensors are usually available in the R&D or vehicle production stage. Note that if Assumption 2 does not hold, the proposed TS fuzzy reduced-order observer design without using neural network is still valid. However, the estimation performance of the NN-based TS fuzzy reduced-order observer is superior over the observer without neural network as demonstrated in Section V.

Consider the following SMO for system (35) used to identify the uncertainty  $d_d$  in the training data:

$$\begin{aligned} \dot{\hat{x}}_d &= \sum_{i=1}^m \rho_i(z) (A_{idd} \hat{x}_d + A_{idq} x_q + L_{di} e_{x_d}) + f_d(x) \\ &\quad + g_d(y, u) - \nu \end{aligned} \quad (36)$$

where  $e_{x_d} = x_d - \hat{x}_d$ ,  $\hat{x}_d$  is the estimate of  $x_d$ , and  $L_{di}$ , for  $i \in \mathbb{I}_m$ , are to be designed. The signal  $\nu$  in (36) is defined as

$$\nu = \begin{cases} -\mu \frac{P_d^{-1} e_{x_d}}{\|e_{x_d}\|}, & \text{if } e_{x_d} \neq 0 \\ 0, & \text{otherwise} \end{cases}$$

where  $\mu > 0$  and  $P_d \in \mathbb{R}^{(n-q) \times (n-q)}$  are to be designed. Note that it is not required to estimate  $x_d$  offline. The estimation  $\hat{x}_d$  of  $x_d$  with SMO (36) is only used to facilitate the

identification of  $d_d$ . From (35) and (36), the dynamics of the SMO estimation error  $e_{x_d}$  is given by

$$\dot{e}_{x_d} = \sum_{i=1}^m \rho_i(z) (A_{idd} - L_{di}) e_{x_d} + d_d + \nu. \quad (37)$$

The following theorem provides sufficient conditions which enable the identification of the uncertainty  $d_d$ .

**Theorem 2.** If there exist matrices  $P_d \succ 0$ ,  $X_{di}$ , for  $i \in \mathbb{I}_m$ , of appropriate dimensions such that the following LMIs hold:

$$\text{He}(P_d A_{idd} - X_{di}) \prec 0 \quad (38)$$

and the scalar  $\mu$  is chosen as

$$\mu = \bar{\mu} + \|P_d\| \bar{d} \quad (39)$$

where  $\bar{\mu}$  is a positive scalar, and  $\bar{d}$  is the bound of  $d_d$ , i.e.,  $\|d_d\| \leq \bar{d}$ . Then, there exists a scalar  $t_{sm} > 0$  such that

$$d_d(t) = -\nu(t), \quad \forall t \geq t_{sm}. \quad (40)$$

Moreover, the observer gains  $L_{di}$ , for  $i \in \mathbb{I}_m$ , in (36) are computed as  $L_{di} = P_d^{-1} X_{di}$ .

*Proof.* Consider the Lyapunov function candidate  $V_d(e_{x_d}) = e_{x_d}^\top P_d e_{x_d}$ . The time-derivative of  $V_d(e_{x_d})$  along the solution of system (37) is given by

$$\begin{aligned} \dot{V}_d(e_{x_d}) &= 2e_{x_d}^\top P_d \left\{ \sum_{i=1}^m \rho_i(z) (A_{idd} - L_{di}) e_{x_d} + d_d + \nu \right\} \\ &= \sum_{i=1}^m \rho_i(z) e_{x_d}^\top \text{He}(P_d A_{idd} - P_d L_{di}) e_{x_d} \\ &\quad - 2\|e_{x_d}\| (\mu - \|P_d\| \|d_d\|). \end{aligned} \quad (41)$$

Since  $X_{di} = P_d L_{di}$ , it follows from (38), (39) and (41) that

$$\dot{V}_d(e_{x_d}) \leq -2\bar{\mu} \|e_{x_d}\|$$

which is the reachability condition [45]. Hence, the sliding motion occurs where  $e_{x_d} = 0$  and  $\dot{e}_{x_d} = 0$ . Assume that sliding motion occurs at  $t = t_{sm} > 0$ , under the sliding motion, it follows from (37) that  $d_d(t) = -\nu(t)$ , for  $\forall t \geq t_{sm}$ .  $\square$

### C. Neural-Network-Based Uncertainty Approximation

The datasets of  $x$ ,  $y$  and  $u$  are collected in various operating conditions of system (3). Using the sliding mode observer (36), the data of the uncertainty  $d_d$  can be identified with expression (40) for each collected dataset. Then, all the datasets of  $y$ ,  $u$  and  $d_d$  are combined into a single dataset, which is used to train the neural network  $\eta_d(y, u)$  to approximate  $d_d$ . To train the neural network  $\eta_d(y, u)$ , where  $\text{col}\{y, u\}$  is the input and  $d_d$  is the output, Matlab Deep Learning Toolbox is used in this paper. Note that to ensure the generalization capability of  $\eta_d(y, u)$  on new data, a part of the combined dataset, e.g., 20%, is reserved for the validation of NN performance. To incorporate the trained neural network  $\eta_d(y, u)$  into the observer (9), we use  $\eta(y, u) = [\eta_d(y, u)^\top \ 0]^\top$ .

**Remark 6.** If the data of  $\omega$  can be also collected, then the data of the uncertainty vector  $d$  can be fully identified. In this

case, the neural network  $\eta(y, u)$  can be trained to approximate  $d$  instead of  $d_d$ .

**Remark 7.** Denote  $\hat{y} = C\hat{x}$  as output of observer (9). Choosing  $H = [I_{n-p} \ 0_{(n-p) \times p}]$ , it follows from (17) that  $M$  is computed as  $M = \begin{bmatrix} I_{n-p} \\ 0_{p \times (n-p)} \end{bmatrix}$ . Hence, it follows from (12) that  $e_y = y - \hat{y} \equiv 0$ . In other words, the output of the observer (9) is identical to the measured output of system (3).

## V. EXPERIMENTAL RESULTS

To validate the practical performance of the proposed TS fuzzy observer scheme, this section provides experimental results carried out with the INSA autonomous vehicle, depicted in Fig. 3(a). The experimental tests are performed on the Gyrovia test track shown in Fig. 3(b), situated at the Transalley technology hub, in Valenciennes, France, which is designed to safely simulate traffic scenarios in an urban environment.



Fig. 3. Experimental test facilities. (a) INSA autonomous vehicle at LAMIH-CNRS laboratory, (b) Gyrovia test track at the Transalley technology hub.

Taking into account the physical limitations during normal driving conditions [22], the vehicle state-space compact set is defined as

$$\mathcal{D} = \{v_y \in [v_y, \bar{v}_y], y_r \in [y_r, \bar{y}_r], v_x \in [v_x, \bar{v}_x]\}$$

where  $v_y = -1.5$  [m/s],  $\bar{v}_y = 1.5$  [m/s],  $y_r = -1.1$  [rad/s] and  $\bar{y}_r = 1.1$  [rad/s], and  $v_x = 1.5$  [m/s],  $\bar{v}_x = 20$  [m/s]. Using the sector nonlinearity method [42] with  $z \in \mathbb{R}^2$ , a four-rule TS fuzzy model of the vehicle system (2) can be easily obtained. Note from the vehicle model (2) that the matrices  $C$  and  $W$  are respectively full row rank and full column rank, and  $\text{rank}(CW) = \text{rank}(W)$ . Moreover,  $C$  and  $W$  are in the form (5) and (32), respectively. Furthermore, from the analytical expression of  $f(x)$  and the vehicle compact set  $\mathcal{D}$ , we can verify that Assumption 1 holds for the vehicle model (2).

Solving the convex optimization problem in Theorem 1, we obtain the following gains for the reduced-order observer (9):

$$G = \begin{bmatrix} 1 & -0.1390 & 0 \end{bmatrix}, \quad M = \begin{bmatrix} 1 \\ 0 \\ 0 \end{bmatrix}, \quad N = \begin{bmatrix} 0.1390 & 0 \\ 1 & 0 \\ 0 & 1 \end{bmatrix}$$

$$\begin{aligned} E_1 = E_2 = -9.8214, & \quad E_3 = E_4 = -130.9522 \\ F_1 = [1.7980 \ 1.1000], & \quad F_2 = [1.7980 \ -1.1000] \\ F_3 = [23.9739 \ 1.1000], & \quad F_4 = [23.9739 \ -1.1000] \end{aligned}$$

with  $\gamma_{\min} = 0.1029$ . Since the last column of  $G$  is 0, it is not necessary to approximate the last component  $d_3$  of the uncertainty vector  $d$  by neural network, *i.e.*, only the first

two components  $d_1$  and  $d_2$  of  $d$  need to be approximated by  $\eta(y, u)$ . To train the neural network  $\eta(y, u)$ , the data are collected with the INSA autonomous vehicle on the Gyrovia test track under various driving scenarios. The driving maneuvers include several driving situations: random smooth driving, driving in a roundabout, taking a sharp turn, making a double lane change, and an extreme driving where the vehicle is driven in an aggressive manner with a rapid lane change and a rapid change of the longitudinal speed. A VBOX III sensor from Racelogic is installed on the vehicle, which comprises a double antennas GPS equipped with RTK correction. It is coupled with a six-degrees-of-freedom inertial measurement unit (IMU) composed by three accelerometers and three gyroscopes. The IMU, dual GPS, and other measurements are processed by a fusion system. Experimental data  $v_y$ ,  $y_r$ ,  $v_x$  and  $\delta$  are logged through CAN busses using a dSpace MicroAutobox II, then transferred to a Host PC for offline analysis as shown in Fig. 4. All the vehicle signals are sampled at 0.01 [s].

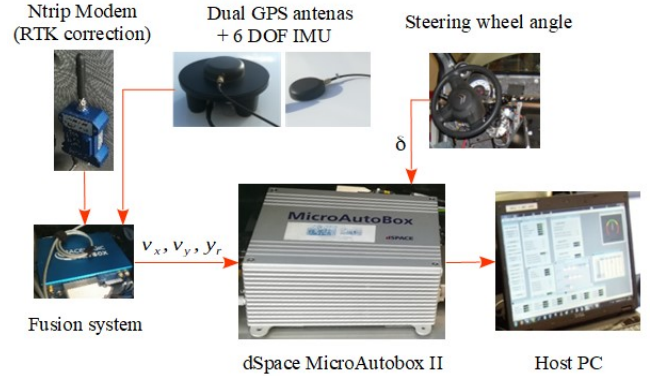


Fig. 4. Vehicle sensors and acquisition system.

The experimental data are separated into a training set and a test set with the ratio 80%–20%. To improve the approximation performance of the trained NNs, we train two separate neural networks  $\eta_1(y, u)$  and  $\eta_2(y, u)$  to approximate  $d_1$  and  $d_2$ , respectively. The same structure is used for both NNs  $\eta_1(y, u)$  and  $\eta_2(y, u)$ , *i.e.*, 1 hidden layer with 5 hidden units and hyperbolic tangent activation functions. This NN structure has been chosen by hyperparameters optimization/exhaustive search. In the following, we consider three test scenarios to illustrate the performance of the proposed NN-based TS fuzzy reduced-order observer as well as the observer without neural network, *i.e.*,  $\eta(y, u) \equiv 0$ . Comparison with the existing TS fuzzy observer in [22] is also provided. Note that the lateral speed is estimated by the estimation scheme [22] with a nominal vehicle model. Hence, the estimation performance of the observer in [22] is similar to that of the proposed TS observer without using neural networks. Note also that a full-order observer has been developed in [22], which requires a higher implementation cost compared to the reduced-order observer in this paper.

### A. Scenario 1: Random Smooth Driving

For this test scenario, the vehicle is driven on a random trajectory with some smooth turns. The vehicle trajectory, longitudinal speed, steering angle and wheel torque are depicted in Figs. 5(a), (b), (c), (d). The estimations by SMO of  $d_1$ ,  $d_2$ , and their NN-based approximations are illustrated in Figs. 5(e) and 5(f). The estimation performance of the proposed TS fuzzy observer with and without including NN-based uncertainty approximations, as well as the nonlinear observer proposed in [22], is demonstrated in Fig. 6. We can see that both TS fuzzy reduced-order observers with and without NNs, as well as the observer [22], perform well in this scenario. However, the NN-based observer generally outperforms the observer without NNs and the TS observer [22], especially when the magnitude of the lateral speed becomes large.

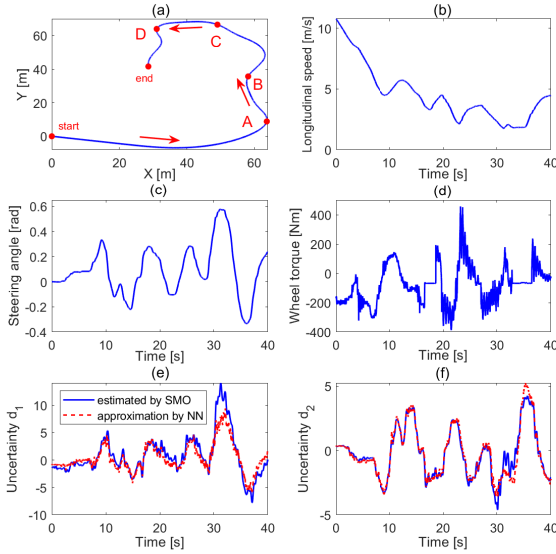


Fig. 5. Driving scenario 1: (a) vehicle trajectory  $X$ - $Y$ , (b) longitudinal speed  $v_x$ , (c) steering angle  $\delta$ , (d) wheel torque  $T_w$ , (e) uncertainty  $d_1$  estimation and its NN-based approximation, (f) uncertainty  $d_2$  estimation and its NN-based approximation.

### B. Scenario 2: Driving with Roundabout and Sharp Turn

The vehicle enters and exits a roundabout then makes a sharp turn in this driving scenario, where the vehicle trajectory, longitudinal speed, steering angle and wheel torque are shown in Figs. 7(a), (b), (c), (d). The estimations by SMO of  $d_1$ ,  $d_2$ , and their NN-based approximations are demonstrated in Figs. 7(e) and (f). The estimation performance of the proposed observer with and without neural networks, as well as the observer [22], is illustrated in Figs. 8. Despite a good estimation of both TS fuzzy reduced-order observers as well as the observer [22], the NN-based observer outperforms the observer without NNs and the observer [22], specifically when the vehicle is driven around the roundabout (or takes a sharp turn) with a large steering angle.

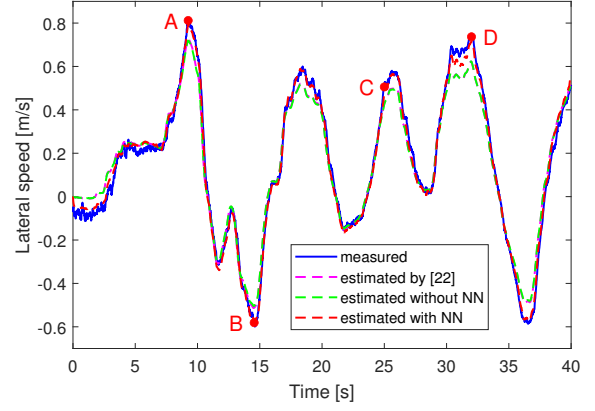


Fig. 6. Driving scenario 1: estimation of the lateral speed  $v_y$  by the TS fuzzy reduced-order observer with and without neural networks, as well as the observer [22].

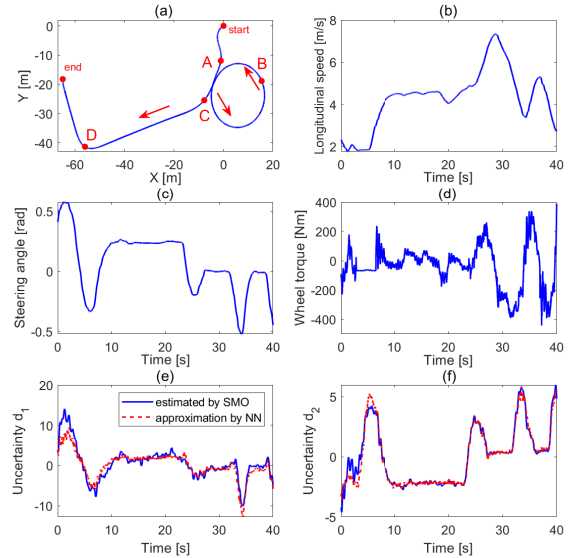


Fig. 7. Driving scenario 2: (a) vehicle trajectory  $X$ - $Y$ , (b) longitudinal speed  $v_x$ , (c) steering angle  $\delta$ , (d) wheel torque  $T_w$ , (e) uncertainty  $d_1$  estimation and its NN-based approximation, (f) uncertainty  $d_2$  estimation and its NN-based approximation.

### C. Scenario 3: Extreme Driving Condition

For this test scenario, the vehicle is driven in a zigzag manner, *i.e.*, extreme driving, where the vehicle trajectory, speed, steering angle and wheel torque are shown in Figs. 9(a), (b), (c), (d). The extreme manner of the driving in this scenario is reflected in a high longitudinal speed profile, quick changes in the steering angle, as well as quick changes in the lateral speed as shown in Fig. 9(b), Fig. 9(c) and Fig. 10, respectively. The estimations of  $d_1$ ,  $d_2$  by SMO, and their NN-based approximations are presented in Figs. 9(e) and (f). The estimation performance of the proposed observer with and without NNs, as well as the observer [22], is illustrated in Fig. 10. We can see that the observer without NNs and the observer [22] poorly perform in this test. It is not the case of the NN-based TS fuzzy observer, which still provides

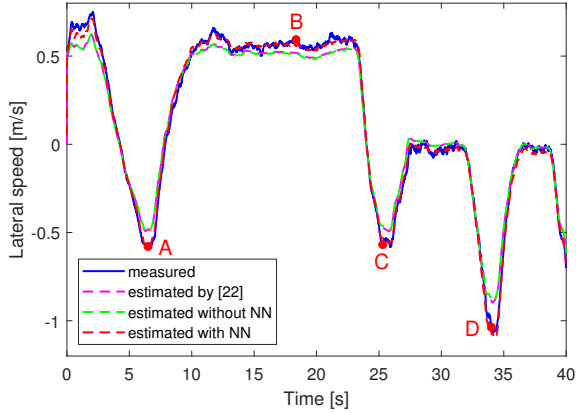


Fig. 8. Driving scenario 2: estimation of the lateral speed  $v_y$  by the TS fuzzy reduced-order observer with and without neural networks, as well as the observer [22].

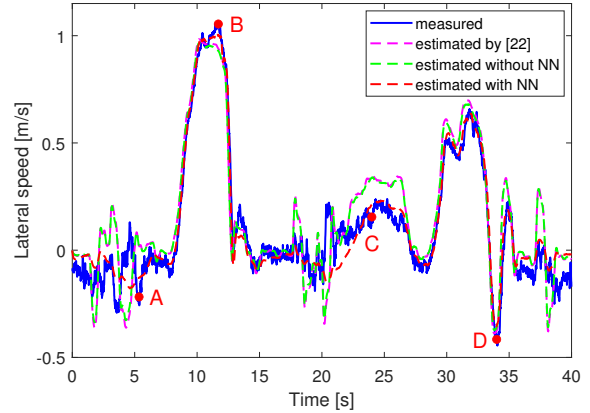


Fig. 10. Driving scenario 3: estimation of the lateral speed  $v_y$  by the TS fuzzy reduced-order observer with and without neural networks, as well as the nonlinear observer [22].

satisfactory estimation performance.

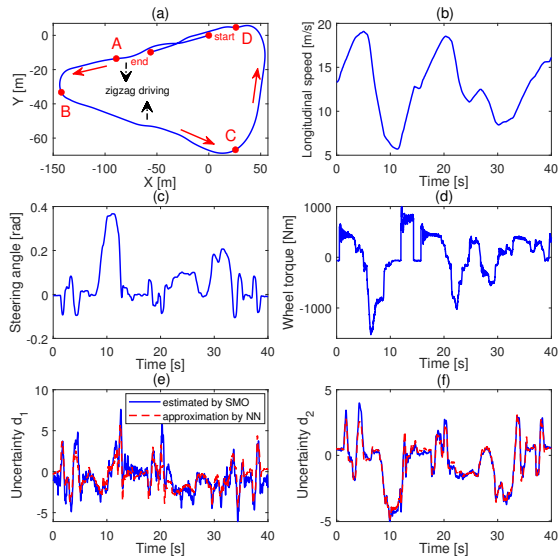


Fig. 9. Driving scenario 3: (a) vehicle trajectory  $X$ - $Y$ , (b) longitudinal speed  $v_x$ , (c) steering angle  $\delta$ , (d) wheel torque  $T_w$ , (e) uncertainty  $d_1$  estimation and its NN-based approximation, (f) uncertainty  $d_2$  estimation and its NN-based approximation.

Quantitative performance comparison in terms of mean absolute estimation error (MAE) of the proposed TS fuzzy reduced-order observers with and without using NNs, as well as the observer [22], for three driving scenarios is provided in Table II. The comparison results further validate the superiority of the NN-based observer over the observer without neural networks as well as the existing method in [22]. It should be also noted that the estimation performance by the observer without NNs and the nonlinear observer in [22] are roughly the same in all scenarios.

**Remark 8.** Experimental results have shown promising performance of the proposed NN-based observer scheme, especially in driving situations where the steering angle becomes

TABLE II  
QUANTITATIVE ESTIMATION PERFORMANCE COMPARISON.

Mean absolute error	Scenario 1	Scenario 2	Scenario 3
Observer [22]	0.0479	0.0501	0.1040
Observer without NNs	0.0484	0.0529	0.0988
NN-based observer	0.0203	0.0198	0.0529

large, *e.g.*, sharp turn, roundabout, etc. In such situations, the small angle assumption and, accordingly, the nominal vehicle model does not hold well due to the presence of large uncertainties. Using neural networks has been shown to be useful in these cases to approximate the modeling uncertainties, and subsequently to mitigate the uncertainty effects on the estimation errors.

## VI. CONCLUDING REMARKS

We have developed a NN-based TS fuzzy reduced-order observer to estimate the vehicle nonlinear dynamics subject to modeling uncertainties and unknown inputs. Motivated by recent advances in NN-based methods, a data-driven approach is proposed to construct NNs, which are used to approximate vehicle dynamics uncertainties. A sliding mode observer is proposed to identify the model uncertainty data from the training data. Then, the NNs are incorporated into the TS fuzzy reduced-order observer, whose design is based on the  $\mathcal{H}_\infty$  filtering method and LMI-based technique. The NN-based uncertainty approximation mitigates the effect of uncertainty on the estimation error. Moreover, the reduced-order observer structure allows reducing the online implementation cost. The estimation performance of the proposed observer scheme has been validated with an autonomous vehicle and a real test track under different driving scenarios. The experimental results have shown a satisfactory performance of the new NN-based observer scheme, especially in situations where the vehicle modeling uncertainties become important due to a large steering angle, *e.g.*, sharp turn, roundabout, etc. Future works focus on using the proposed NN-based TS fuzzy observer for output feedback vehicle control in extreme driving scenarios.

## REFERENCES

- [1] L. Li, D. Wen, N.-N. Zheng, and L.-C. Shen, "Cognitive cars: A new frontier for ADAS research," *IEEE Trans. Intell. Transp. Syst.*, vol. 13, no. 1, pp. 395–407, 2012.
- [2] R. Rajamani, *Vehicle Dynamics and Control*. Springer Science & Business Media, 2011.
- [3] B. Lenzo, M. Zanchetta, A. Sorniotti, P. Gruber, and W. De Nijs, "Yaw rate and sideslip angle control through single input single output direct yaw moment control," *IEEE Trans. Control Syst. Technol.*, vol. 29, no. 1, pp. 124–139, 2021.
- [4] J. Liu, Q. Dai, H. Guo, J. Guo, and H. Chen, "Human-oriented online driving authority optimization for driver-automation shared steering control," *IEEE Trans. Intell. Veh.*, vol. 7, no. 4, pp. 863–872, 2022.
- [5] H. Zhang, X. Huang, J. Wang, and H. Karimi, "Robust energy-to-peak sideslip angle estimation with applications to ground vehicles," *Mechatronics*, vol. 30, pp. 338–347, 2015.
- [6] M. Doumiati, A. C. Victorino, A. Charara, and D. Lechner, "Onboard real-time estimation of vehicle lateral tire-road forces and sideslip angle," *IEEE/ASME Trans. Mechatron.*, vol. 16, pp. 601–614, 2011.
- [7] K. Nam, S. Oh, H. Fujimoto, and Y. Hori, "Estimation of sideslip and roll angles of electric vehicles using lateral tire force sensors through RLS and Kalman filter approaches," *IEEE Trans. Ind. Electron.*, vol. 60, no. 3, pp. 988–1000, 2013.
- [8] J. Pan, A.-T. Nguyen, T.-M. Guerra, C. Sentouh, S. Wang, and J.-C. Popieul, "Vehicle actuator fault detection with finite-frequency specifications via Takagi-Sugeno fuzzy observers: Theory and experiments," *IEEE Trans. Veh. Technol.*, vol. 72, no. 1, pp. 407–417, 2023.
- [9] J. Liu, Z. Wang, L. Zhang, and P. Walker, "Sideslip angle estimation of ground vehicles: A comparative study," *IET Control Theory Appl.*, vol. 14, no. 20, pp. 3490–3505, 2020.
- [10] D. Chindamo, B. Lenzo, and M. Gadola, "On the vehicle sideslip angle estimation: a literature review of methods, models, and innovations," *Appl. Sci.*, vol. 8, no. 3, pp. 1–20, 2018.
- [11] H. Guo, Z. Yin, D. Cao, H. Chen, and C. Lv, "A review of estimation of vehicle tire-road interactions toward automated driving," *IEEE Trans. Syst., Man, Cybern.: Syst.*, vol. 49, no. 1, pp. 14–30, 2019.
- [12] W. Chen, D. Tan, and L. Zhao, "Vehicle sideslip angle and road friction estimation using online gradient descent algorithm," *IEEE Trans. Veh. Technol.*, vol. 67, no. 12, pp. 475–485, 2018.
- [13] E. Hashemi, M. Pirani, A. Khajepour, B. Fidan, A. Kasaiezadeh, and S. Chen, "Opinion dynamics-based vehicle velocity estimation and diagnosis," *IEEE Trans. Intell. Transp. Syst.*, vol. 19, pp. 142–148, 2018.
- [14] D. Selmanaj, M. Corno, G. Panzani, and S. Savaresi, "Vehicle sideslip estimation: A kinematic based approach," *Control Eng. Pract.*, vol. 67, pp. 1–12, 2017.
- [15] A.-T. Nguyen, T.-M. Guerra, C. Sentouh, and H. Zhang, "Unknown input observers for simultaneous estimation of vehicle dynamics and driver torque: Theoretical design and hardware experiments," *IEEE/ASME Trans. Mechatron.*, vol. 24, no. 6, pp. 2508–2518, 2019.
- [16] X. Xia, L. Xiong, Y. Lu, L. Gao, and Z. Yu, "Vehicle sideslip angle estimation by fusing inertial measurement unit and global navigation satellite system with heading alignment," *Mech. Syst. Signal Process.*, vol. 150, pp. 1–18, 2021.
- [17] Z. Wang, X. Zhou, and J. Wang, "Extremum-seeking-based adaptive model-free control and its application to automated vehicle path tracking," *IEEE/ASME Trans. Mechatron.*, vol. 27, no. 5, pp. 874–884, 2022.
- [18] X. Li, C. Chan, and Y. Wang, "A reliable fusion methodology for simultaneous estimation of vehicle sideslip and yaw angles," *IEEE Trans. Veh. Technol.*, vol. 65, no. 6, pp. 4440–4458, 2016.
- [19] S. Cheng, L. Li, and J. Chen, "Fusion algorithm design based on adaptive SCKF and integral correction for side-slip angle observation," *IEEE Trans. Ind. Electron.*, vol. 65, no. 7, pp. 5754–5763, 2018.
- [20] X. Xia, P. Hang, N. Xu, Y. Huang, L. Xiong, and Z. Yu, "Advancing estimation accuracy of sideslip angle by fusing vehicle kinematics and dynamics information with fuzzy logic," *IEEE Trans. Veh. Technol.*, vol. 70, no. 7, pp. 6577–6590, 2021.
- [21] R. Song and Y. Fang, "Vehicle state estimation for INS/GPS aided by sensors fusion and SCKF-based algorithm," *Mech. Syst. Signal Process.*, vol. 150, p. 107315, 2021.
- [22] A.-T. Nguyen, T.-Q. Dinh, T.-M. Guerra, and J. Pan, "Takagi-Sugeno fuzzy unknown input observers to estimate nonlinear dynamics of autonomous ground vehicles: Theory and real-time verification," *IEEE/ASME Trans. Mechatron.*, vol. 26, no. 3, pp. 1328–1338, 2021.
- [23] H. Grip, L. Imsland, T. Johansen, J. Kalkkuhl, and A. Suissa, "Vehicle sideslip estimation: Design, implementation, and experimental validation," *IEEE Control Syst.*, vol. 29, no. 5, pp. 36–52, 2009.
- [24] B. Zhang, H. Du, J. Lam, N. Zhang, and W. Li, "A novel observer design for simultaneous estimation of vehicle steering angle and sideslip angle," *IEEE Trans. Ind. Electron.*, vol. 63, no. 7, pp. 4357–4366, 2016.
- [25] X. Ding, Z. Wang, and L. Zhang, "Event-triggered vehicle sideslip angle estimation based on low-cost sensors," *IEEE Trans. Indus. Inform.*, vol. 18, no. 7, pp. 4466–4476, 2022.
- [26] Q. Zhang, H. Jing, Z. Liu, Y. Jiang, and M. Gu, "A novel PWA lateral dynamics modeling method and switched T-S observer design for vehicle sideslip angle estimation," *IEEE Trans. Indus. Electron.*, vol. 69, no. 2, pp. 1847–1857, 2022.
- [27] K. Hornik, "Approximation capabilities of multilayer feedforward networks," *Neural Netw.*, vol. 4, no. 2, pp. 251–257, 1991.
- [28] X. Ji, X. He, C. Lv, Y. Liu, and J. Wu, "Adaptive-neural-network-based robust lateral motion control for autonomous vehicle at driving limits," *Control Eng. Pract.*, vol. 76, pp. 41–53, 2018.
- [29] R. Rahimilarki, Z. Gao, A. Zhang, and R. Binns, "Robust neural network fault estimation approach for nonlinear dynamic systems with applications to wind turbine systems," *IEEE Trans. Ind. Informat.*, vol. 15, no. 12, pp. 6302–6312, 2019.
- [30] W. Jeon, A. Chakrabarty, A. Zemouche, and R. Rajamani, "Simultaneous state estimation and tire model learning for autonomous vehicles," *IEEE/ASME Trans. Mechatron.*, vol. 26, no. 4, pp. 1941–1950, 2021.
- [31] Z. Peng, J. Wang, and J. Wang, "Constrained control of autonomous underwater vehicles based on command optimization and disturbance estimation," *IEEE Trans. Indus. Electron.*, vol. 6, no. 5, pp. 27–35, 2019.
- [32] H. Taghavifar, C. Hu, Y. Qin, and C. Wei, "EKF-neural network observer based type-2 fuzzy control of autonomous vehicles," *IEEE Trans. Intell. Transp. Syst.*, vol. 22, no. 8, pp. 4788–4800, 2021.
- [33] Y. Xing and C. Lv, "Dynamic state estimation for the advanced brake system of electric vehicles by using deep recurrent neural networks," *IEEE Trans. Indus. Electron.*, vol. 67, no. 11, pp. 9536–9547, 2020.
- [34] B. Boada, M.-J. Boada, L. Vargas-Melendez, and V. Diaz, "A robust observer based on  $\mathcal{H}_\infty$  filtering with parameter uncertainties combined with neural networks for estimation of vehicle roll angle," *Mech. Syst. Signal Process.*, vol. 99, pp. 611–623, 2018.
- [35] B. Boada, M.-J. Boada, A. Gauchia, E. Olmeda, and V. Diaz, "Sideslip angle estimator based on ANFIS for vehicle handling and stability," *J. Mech. Sci. Technol.*, vol. 29, no. 4, pp. 1473–1481, 2015.
- [36] S. Melzi and E. Sabbioni, "On the vehicle sideslip angle estimation through neural networks: Numerical and experimental results," *Mech. Syst. Signal Process.*, vol. 25, no. 6, pp. 2005–2019, 2011.
- [37] T. Novi, R. Capitani, and C. Annicchiarico, "An integrated artificial neural network–unscented Kalman filter vehicle sideslip angle estimation based on inertial measurement unit measurements," *J. Automobile Eng.*, vol. 233, no. 7, pp. 1864–1878, 2019.
- [38] W. Wei, B. Shaoyi, Z. Lanchun, Z. Kai, W. Yongzhi, and H. Weixing, "Vehicle sideslip angle estimation based on general regression neural network," *Math. Problems Eng.*, vol. 2016, pp. 1–7, 2016.
- [39] D. Kim, K. Min, H. Kim, and K. Huh, "Vehicle sideslip angle estimation using deep ensemble-based adaptive Kalman filter," *Mech. Syst. Signal Process.*, vol. 144, pp. 1–17, 2020.
- [40] T. Graber, S. Lupberger, M. Unterreiner, and D. Schramm, "A hybrid approach to sideslip angle estimation with recurrent neural networks and kinematic vehicle models," *IEEE Trans. Intell. Veh.*, vol. 4, no. 1, pp. 39–47, 2019.
- [41] C. Edwards and S. K. Spurgeon, *Sliding Mode Control: Theory and Applications*. Taylor & Francis, 1998.
- [42] K. Tanaka and H. Wang, *Fuzzy Control Systems Design and Analysis: a Linear Matrix Inequality Approach*. John Wiley & Sons, 2004.
- [43] A. Zemouche, M. Boutayeb, and I. Bara, "Observers for a class of Lipschitz systems with extension to  $\mathcal{H}_\infty$  performance analysis," *Syst. Control Lett.*, vol. 57, no. 1, pp. 18–27, 2008.
- [44] H. Trinh and T. Fernando, *Functional Observers for Dynamical Systems*. Berlin: Springer, 2012.
- [45] C. M. Nguyen, C.-P. Tan, and H. Trinh, "Sliding mode observer for estimating states and faults of linear time-delay systems with outputs subject to delays," *Automatica*, vol. 124, p. 109274, 2021.



**Cuong M. Nguyen** received the B.Sc. and M.Sc. degrees in Mathematics from Vietnam National University, Hanoi, Vietnam. In 2017, he received the Ph.D. degree from School of Engineering, Deakin University, Australia, where he further worked as postdoc and lecturer for several years. He is currently a postdoc in Autonomous Vehicles at LAMIH UMR CNRS 8201, Université Polytechnique Hauts-de-France, France. His research interests lie in the areas of Control Systems, Machine Learning, and Optimization.



**Anh-Tu Nguyen** (M'18, SM'21) is an Associate Professor at the INSA Hauts-de-France, Université Polytechnique Hauts-de-France, Valenciennes, France. He received the degree in engineering and the M.Sc. degree in automatic control from Grenoble Institute of Technology, Grenoble, France, in 2009, and the Ph.D. degree in automatic control from the University of Valenciennes, Valenciennes, France, in 2013. He is an Associate Editor for the IEEE Transactions on Intelligent Transportation Systems, the IFAC journal Control Engineering Practice, the IET

Journal of Engineering, the SAE International Journal of Vehicle Dynamics, Stability, and NVH, the Springer Automotive Innovation, Frontiers in Control Engineering, and a Guest Editor for special issues in various international journals. His research interests include robust control and estimation, cybernetics control systems, human-machine shared control with a strong emphasis on mechatronics applications.



**Sébastien Delprat** received the Ph.D. degree in 2002 from the University of Valenciennes and Hainaut Cambrésis, Valenciennes, France, where he became an Assistant Professor. Since 2012, he has been a Full Professor. His research interests include vehicle control, and especially hybrid vehicle energy management.